

EXPERIMENTAL INVESTIGATION ON HOT CORROSION BEHAVIOUR OF UNCOATED AND CERMETS COATED SUPERCO-605.

Vinod Kumar M S¹, R Suresh¹, N Jegadeeswaran²

¹Department of Mechanical Engineering, VTU-CPGS, Mysuru-570029, Karnataka, India

² School of Mechanical engineering, REVA University, Bangalore-560065, Karnataka, India.

*Corresponding author Email: vinod.sadashiv@gmail.com

Co authors Email: drsureshvtu@gmail.com , njagadeeswaran@reva.edu.in

Abstract

Superalloy turbine parts work at high temperatures and in harsh chemical environments that wear down the surfaces of the parts, which causes the turbine part to degrade. A protective coating of cermets is applied to the substrate materials to shield the surface of the turbine components from the harsh working environment. In the present research, the carbide alloy powder (WC-Co+70%NiCrBSi) is coated on the substrate Superco-605 super alloy using the High-velocity oxygen fuel (HVOF) spray coating technique after which both uncoated and coated Superco-605 samples were subjected to hot corrosion investigations in the presence of (Na₂SO₄+60% V₂O₅) molten salt for 50 cycles at 700 °C. The microstructural investigation of all the hot corroded specimens were performed using SEM / EDS techniques, which confirms that the oxide scale formed in the case of coated sample is protective and it can prevent the penetration of reaction products that can attack the substrate.

Key words: Superc-605; HVOF spray coating;; Hot corrosion; Cermets; Superalloys; turbine blades.

1. Introduction

Our daily existence has grown increasingly reliant on the steady flow of electricity in recent years. In scenarios involving life support systems, air traffic, and trains, even a minor disruption in the power supply causes significant turmoil and occasionally leads to a fatality. Although there are backup facilities, it is preferable to maintain a constant source of electricity. The most common way of producing electricity is thermal power production, which employs gas turbines to power electrical generators.²⁻³

High operating temperatures—typically greater than 600 °C—are applied to the gas turbine parts. Due to the reaction products created by burning coal and the high temperatures in this area, the turbine blades are vulnerable to hot corrosion and erosion, which undoubtedly shortens the component's life expectancy.⁴⁻⁵ Better alloy systems (steel, titanium alloys, and superalloys) have been developed as a consequence of the rising need for suitable materials to accomplish the necessary performance.⁶⁻⁸ Superalloys are strong at high temperatures, according to several studies, however it may be preferable to prevent hot corrosion and erosion of superalloys by properly covering the superalloy's substrate.⁹⁻¹¹ One of the greatest options for superalloys to withstand high operating temperatures and also to prevent material deterioration by hot corrosion and erosion was determined to be using cermets as coating composition. ¹²⁻¹⁴

The most used spray coating technique is HVOF because it creates a coating with less porosity and a strong bond between the coated layer and the base metal.¹⁵⁻¹⁷ The most significant type of corrosion occurs when materials exposed to that environment, such as fuel or air, are subjected to alkali salt contamination when a turbine is operating.¹⁸ It is crucial to understand how blade materials degrade and to defend the value of alloying elements, which are responsible for the formation of oxide layer and can shield the base metal from hot corrosion.¹⁹⁻²¹

According to a study, the alloying components of the coating were chosen so that when they interact with one another in the working environment, they should be able to form a long-lasting protective layer that gives resistance to high temperature corrosion.²³⁻²⁴

Jagadeeswaran et al. reported the investigation on high-temperature corrosion of untreated and coated Superco-605 samples at 800 °C. The results of this investigation show that the HVOF spray deposition is efficient in increasing resistance to heat corrosion since coated samples gain less weight than untreated samples do. The substrate is protected from heat corrosion by a layer rich in alumina at the interface and a chromium-depleted zone toward the top of the oxide scale.²⁵ Zhou et al in a study the substrate was coated with Cr₃C₂-WC-NiCoCrMo and Cr₃C₂-20(NiCr), and studies of high-temperature corrosion is performed at 500 °C in the presence of NaCl-KCl-Na₂SO₄ salt. When the resistance against high temperature corrosion was evaluated using the scale thickness that had formed, it was discovered that the thickness of the Cr₃C₂-WC-NiCoCrMo coating was one-third that of the Cr₃C₂-20(NiCr), and resistance against hot corrosion is improved as a result of the formation of oxides of coating elements.²⁶ Kushal et al. deposited Ni₂₀Cr on boiler steel using the HVOF technology and high temperature corrosion findings revealed that Ni₂₀Cr coating may give great resistance to hot corrosion.²⁷ The current work focuses on coating the cobalt-based superalloy Superco-605 with WC-Co+70 Wt% NiCrBSi and conducting a study on high temperature corrosion in an atmosphere of Na₂SO₄+60% V₂O₅ salt to compare the effects of the coating on the substrate in order to prevent hot corrosion. Based on the conducted literature survey It is observed that there is minimum available literature on the evaluation of high-temperature corrosion behavior of Superco-605 coated with WC-Co+ 70%NiCrBSi.

2. Experimental work

2.1. Superalloy material

The special alloy Superco-605, which is based on Cobalt element, was chosen as the superalloy for the current research project (ASTM B338 Grade 5). According to Table 1, which details the substrate's composition as provided by the supplier and verified by XRD and SEM/EDS analysis, the Cobalt based Superco-605 is most suitable for use in gas and chemical pumps as well as gas turbine blades. The Hyderabad-based company M/S Midhani procured the super alloy, For experimental purposes it was provided in sheets of 5 mm thickness that were then cut into 25 x 25 mm coupons using a wire EDM machine. To ensure adequate adherence of the coating with the substrate, the superalloy samples are grit blasted with alumina. The samples are also dried in hot air to eliminate any moisture content that may be present.

Table 1. Specifications of substrate material

Substrate	Percentage of different elements						
	Cr	Ni	Fe	C	Mn	Si	Co
Superco -605 (ASTM B338 Grade 5)	19	9.8	3.2	0.07	1.48	0.29	Bal

2.2 coating powder

Based on a review of the literature, it was determined to choose cermet coating powder for turbine applications since cermets have been shown to boost resistance to hot corrosion and erosion²⁸. For the current work, carbide alloy powder WC-Co+70 wt% NiCrBSi cermets was used. The supplier's description of the coating powder's composition, which was later validated by XRD and SEM/EDS analysis, is displayed in Table 2. Here, the principal component of the mechanically mixed, irregularly shaped carbide alloy powder is 70% NiCrBSi alloy and 30% WC-Co. The powder particles in this area range in size from $45 \pm 15\mu\text{m}$. Figure 1 displays the results of the SEM and EDS examination of the powdered carbide alloy. It firmly supports the irregular form of the powder particles, and EDS analysis supports the composition of the cermet powder.

Table 2. Specifications of the coating powder.

Sl.No	coating	Alloying elements	Particle Shape	Particle size
1	cermets	WC-Co +70% NiCrBSi	irregular	45 $\pm 15\mu\text{m}$

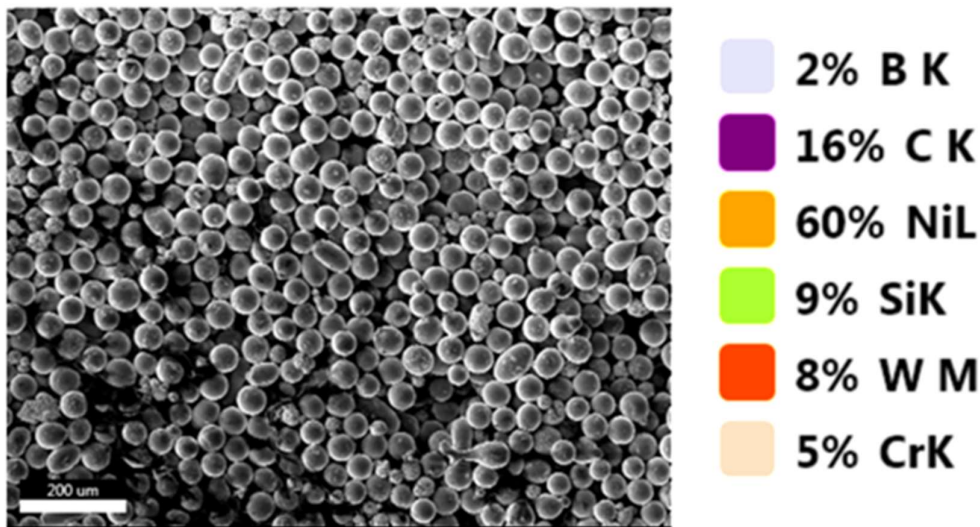


Fig.1. SEM/EDS analysis of WC-Co+70% NiCrBSi cermets.

2.3 HVOF spray coating process

Here, the principal component of the mechanically mixed, irregularly shaped carbide alloy powder is 70% NiCrBSi alloy and 30% WC-Co. The powder particles in this area range in size from $45 \pm 15 \mu\text{m}$. Figure 1 displays the results of the SEM and EDS examination of the powdered carbide alloy. It firmly supports the irregular form of the powder particles, and EDS analysis supports the composition of the cermet powder. The process parameters set for coating deposition are as shown in table 3. The SEM micrograph of the WC-Co+70% NiCrBSi coating on the Ti-31 substrate is shown in Figure 2. From the picture, it can be seen that the coating's microstructure on both substrates is made up of melted and unmelted particles, and that a small amount of porous region is present.

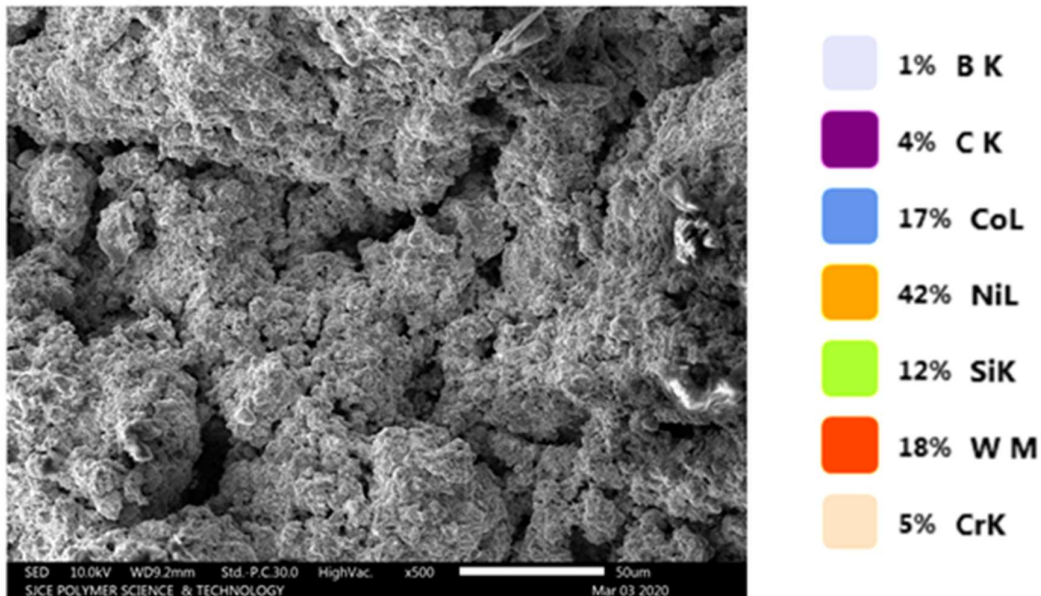


Fig.2. SEM with EDS analysis of WC-Co+NiCrBSi coating on substrate Superco-605.

Table 3. Selected parameters for HVOF spray coating process.

Parameter	Set value
Flow rate of Oxygen in Lpm	251
Feed rate of coating Powder in N/min	0.29-0.49
Flow rate of Fuel in Lpm	54-76
Pressure of Nitrogen gas in N/m^2	49.03×10^4
Flow rate of air in Lpm	698
Distance of sample from spray gun	0.21-0.26 m
Pressure of Fuel in N/m^2	67.03×10^4
Pressure of Oxygen in N/m^2	97.8×10^4

Pressure Air in N/m^2

54.02×10^4

2.3.1 Measurement of coating thickness, density & porosity of coating

The SEM analysis along the cross-section of the coated specimens was utilized to quantify coating thickness, and Table 4 summarizes the properties of the coatings as they were sprayed. The coating thickness values that were measured range from 261 to 296 μm in reference to Figure 3. the density of coated samples is determined using water immersion method, and the density value ranges from 1.125 to 1.196 gm/cm^3 . The surface porosity of the coating was measured. Using a porosity measurement system in line with ASTM B276 standards and the results for the measured porosity percentage fell between 1.12 and 1.38%.

Table.4. Properties of as sprayed coating.

Cermets powder deposited	Average thickness (μm)	Porosity %	Density (gm/cm^3)
Carbide alloy powder WC-Co+70 Wt.%NiCrBSi	275	1.19	1.185

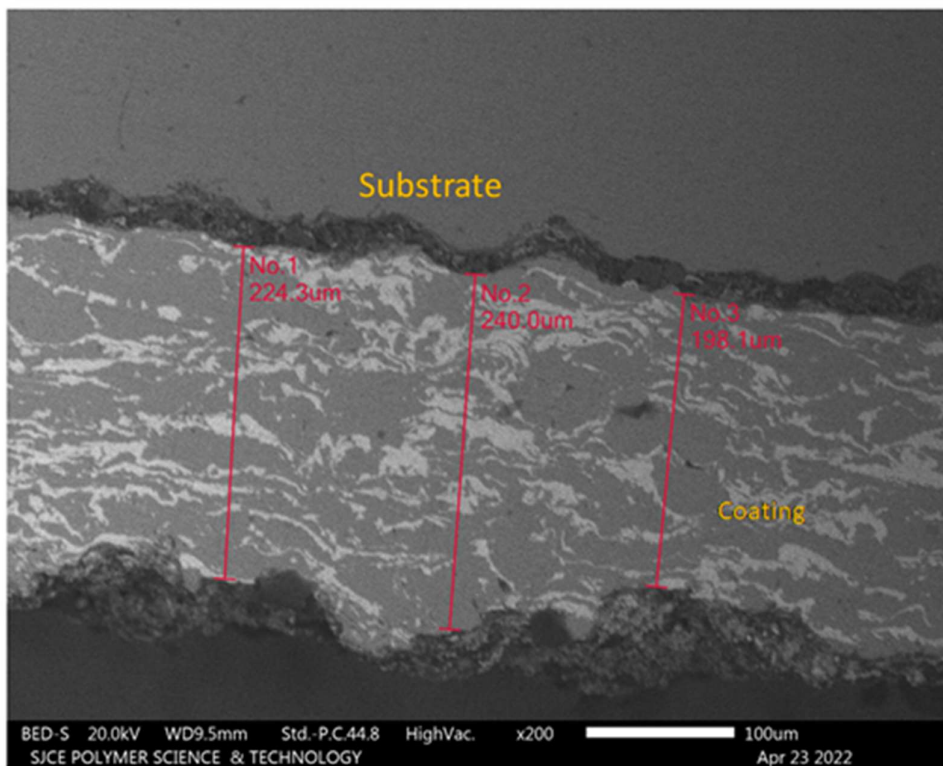


Fig. 3. SEM micrograph of coating cross section of WC-Co +70%NiCrBSi coated Superco-605.

2.3.2 Micro hardness analysis

Micro hardness of the samples was measured using a BUEHLER instrument in accordance with ASTM E384 standards. Micro hardness values were calculated throughout the coated sample's cross section. 1000 gm loads are used during testing on substrate materials and coatings that have been sprayed. And the micro hardness profile of the coatings is depicted in

Fig. 4 as a function of distance from the coating-substrate interface. The micro hardness values for the substrate and coating are shown in Tables 5. Over the cross section, the micro hardness of the coatings is shown to fluctuate, with values significantly increasing closer to the coating-substrate contact and on the coating.

Table5 Micro hardness value across the cross section of coated sample

Sl. No.	Material	Microhardness (Hv)
1	Substrate: Superco-605	285-395
2	Coating : WC-Co+70%NiCrBSi	525-608

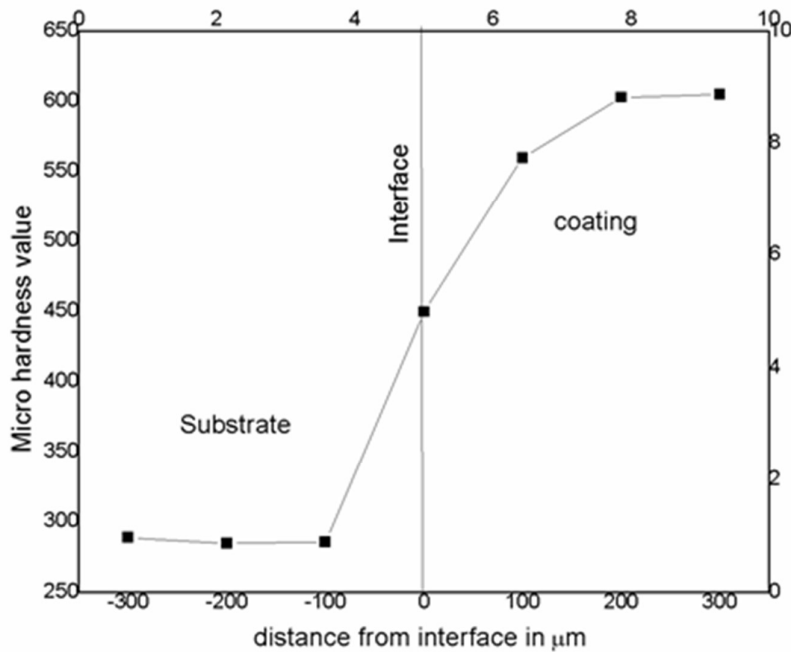


Fig. 4. Micro hardness profiles of as sprayed WC-Co+70% NiCrBSi coating coatings on the substrate Superco-605 superalloy.

2.4 Cyclic studies of hot corrosion

The sample must be cleaned with an acetone solution to remove dirt particles and dried in hot air to eliminate moisture before being used for hot corrosion studies. A silicon carbide tube furnace is used for the hot corrosion test, and it is outfitted with a temperature indicator with a $\pm 5^\circ$ precision made by Electromek in India. Using a camel hair brush, the salt $\text{Na}_2\text{SO}_4+60\%\text{V}_2\text{O}_5$ is applied to the surface of each sample in order to produce a distribution of 3-5 mg/cm². For high temperature cyclic corrosion investigations, these produced specimens were put in an aluminum boat and warmed to keep the weight constant. They were then put in the hot part of the tube furnace, which is maintained at a temperature of 700 °C. For the purpose of researching corrosion kinetics, the boat along with the sample was weighed exactly again after an hour using an electronic scale. Additionally, ocular observations were taken for colour changes. In the current study, each sample is subjected to 50 cycles of hot corrosion, which

include the development of oxide scale, lustre, and cracks. Following 50 cycles of hot corrosion exposure on the samples, XRD, SEM, and EDS methods are used to examine the surface morphology, hot corrosion reaction products, and elements on the oxide scale so obtained.

3. Experimental results and analysis

3.1.1 Visual observations

Figure 5 shows the macrograph of the specimens which are exposed to hot corrosion conditions. In the case of Superco-605 Initially, the uncoated Superco-605 (Ref Fig 5a) specimen was grey in color. After 50 heating cycles due to oxide scale formation, the surface appeared dark grey in color. The oxide scale developed was spalling and cracks started to appear from the 12th cycle onwards of the hot corrosion test. And the sample was undergoing severe sputtering during the study due to which the gain in weight is not significant. For WC-Co+70 Wt. % NiCrBSi coated Superco-605 specimens during 50 hot corrosion cycles, the formation of oxide scale was noted in the initial cycle of hot corrosion itself, the oxide scale developed took on a greenish colour starting with the 25th cycle and the scale obtained was well intact with the base metal and no crack formation was observed at the end of 50 cycles (Ref Fig 5b).

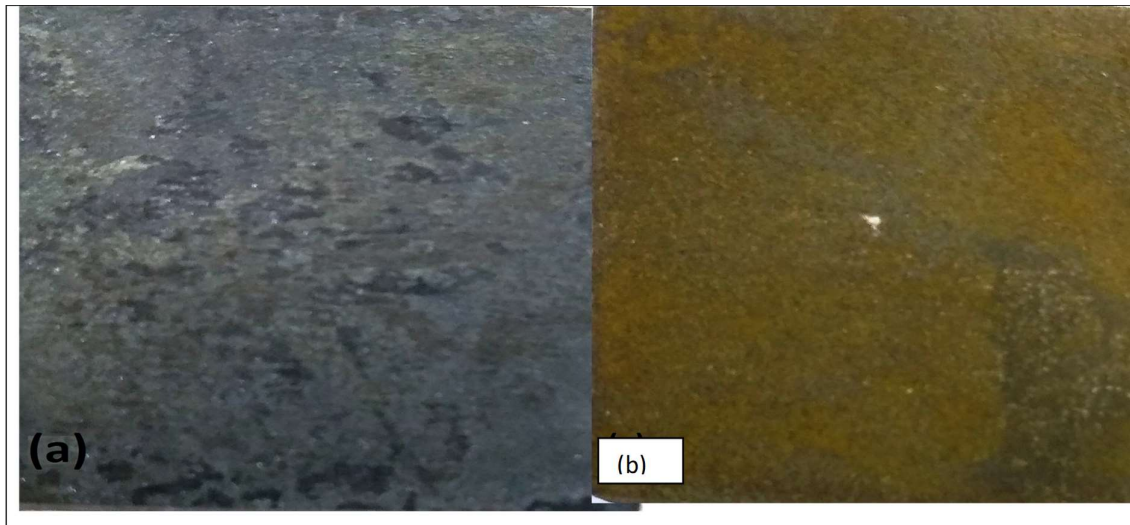


Fig.5. Macro graph of samples subjected to hot corrosion (a) Uncoated Superco-605 (b) WC-Co+ 70 Wt. % NiCrBSi coated Superco-605.

3.1.2 Thermo gravimetric study

Figure 5 depicts the results of the thermo gravimetric study of uncoated and HVOF spray coated samples. From the graph, it is observed that after 50 heating cycles in the presence of Na₂SO₄+ 60 Wt.%V₂O₅ salt, the total weight gain per unit area is used as the parameter to compare the corrosion rate of both the samples under similar test conditions, from the plot it can be observed that the weight gain of coated sample is higher and continuous with the increase in number of heating cycles, where as the weight gain of uncoated sample was rising initially but settles to a constant value during subsequent cycles and since the sample was undergoing spalling and sputtering weight gain of uncoated sample is less than coated sample. The total weight gain after completion 50 cycles of hot corrosion is 3.8 mg/cm² and 7.8

mg/cm² for uncoated and WC-Co+70 Wt.% NiCrBSi coated Superco-605 samples respectively. Figure 6 depicts the trend of square of weight gain per unit area against the number of cycle's shows a divergence from the parabolic rate law for uncoated sample. The corrosion constant K_p is determined from the slope of the linear regression approach. The determined values of K_p are 10.97×10^{-8} and 0.0318×10^{-8} for uncoated and WC-Co+70 Wt.% NiCrBSi coated Superco-605 respectively.

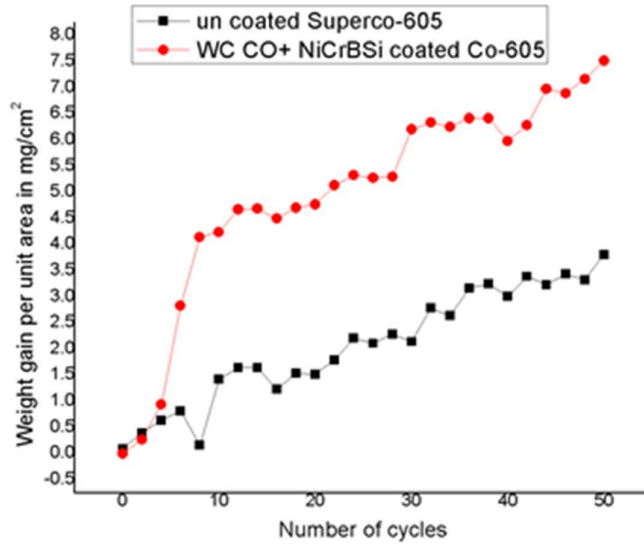


Fig.5. Plot of Weight gain number of cycles of the uncoated and WC-Co+ 70 Wt.% NiCrBSi coated superalloy exposed to hot corrosion.

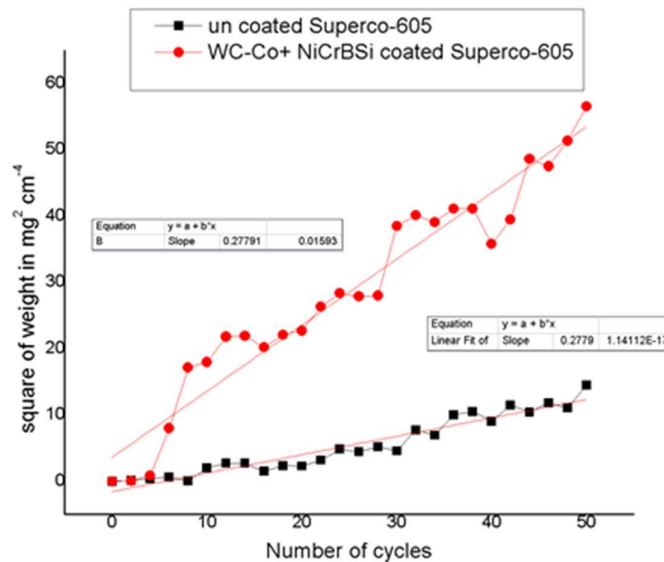


Fig.6.plot of square of weight gain per unit area against Number of cycles of the samples subjected to hot corrosion.

3.1.3 Characterization of corroded samples using SEM with EDS technique

Figure 7a shows SEM with EDS analysis of the oxide scale developed on the uncoated Superco-605 sample after being exposed to 50 heating cycles at 700 °C. The surface morphology shows that the developed oxide scale is flaky and discontinuous, which is a favorable condition for continuous hot corrosion. From the EDS examination at the chosen point, the reaction products of hot corrosion identified are 33% of Na , 33% Co, 18-28% O, 10.12-13.94% S and 4.91% of Co as the major constituents, and Figure 7b shows SEM with EDS analysis of the oxide scale formed on the coated Superco-605 sample exposed to 50 cyclic studies of hot corrosion. Here, the surface morphology indicates that the developed oxide scale is compact and continuous, which protects the substrate from hot corrosion. The EDS examination of the corroded surface shows that the oxide layer formed consists of 11.89% Na, 15.59% V, and 4.62% Co 8.94%W, and 18.43% Ni as reaction products of hot corrosion.

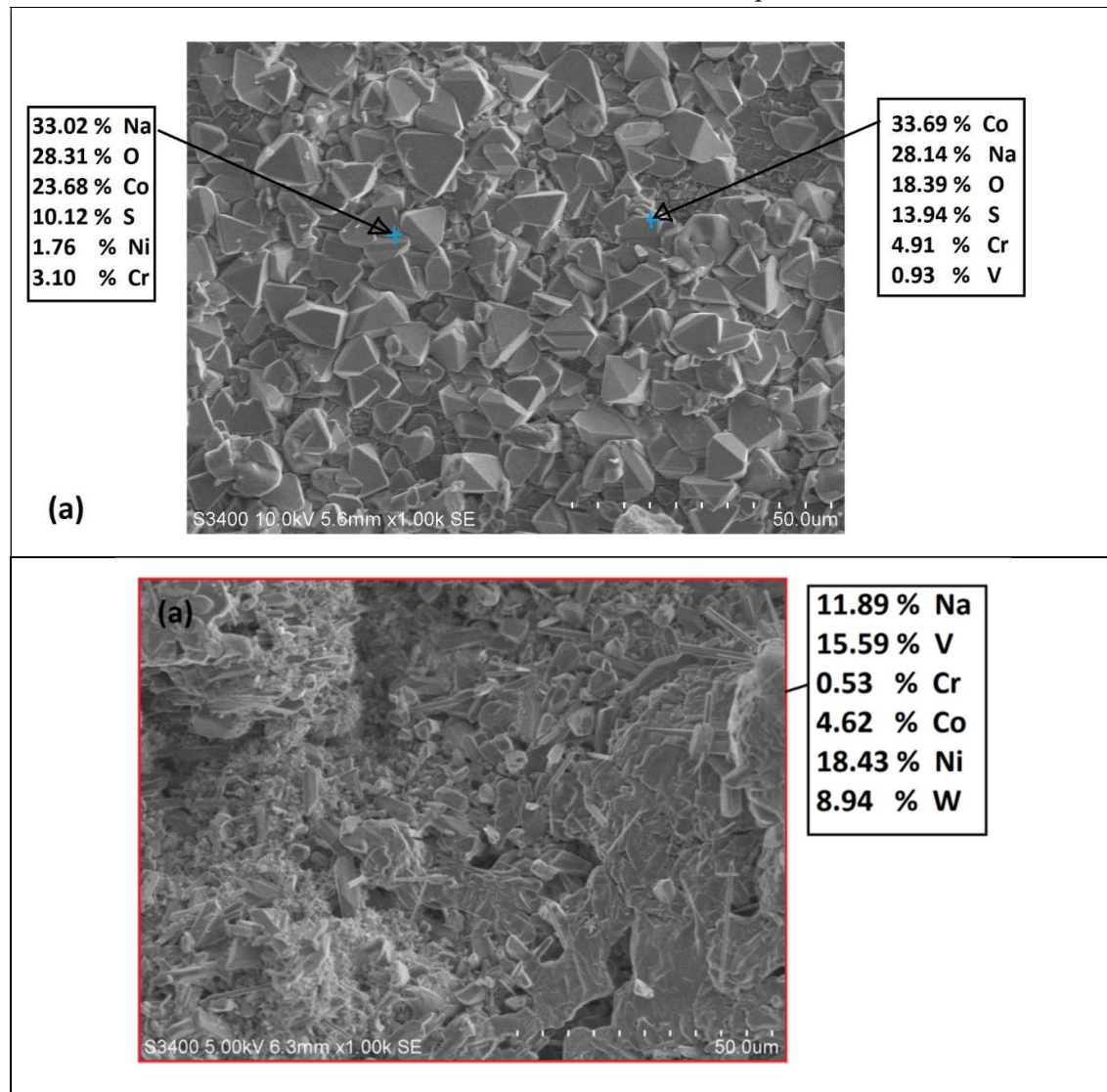


Fig.7. SEM with EDS analysis of uncoated samples exposed to hot corrosion environment. (a) Uncoated Ti-31 (b) WC-Co+ 70 Wt.% NiCrBSi coated Superco-605.

3.1.4 XRD Analysis

X Ray Diffraction analysis of uncoated sample is shown in figure 8 and WC-Co+ 70 Wt. % NiCrBSi coated Superco-605 samples XRD pattern is as shown in figure 9. XRD patterns of uncoated sample exhibits Cr₁₀O₄V₁ as major phases and Fe₂O₄V₁ as minor phases on the corroded surface. Where as in case of the WC-Co+ 70 Wt. % NiCrBSi coated Superco-605 sample the XRD patterns confirm the presence of WC, oxides of Ni, Cr and B as major crystalline phase and, Ti and Si as minor phases on the surface of coated sample subjected to hot corrosion. The oxides of the active elements of coating are beneficial in preventing penetration of reaction products of hot corrosion in to substrate, and improve resistance against hot corrosion.

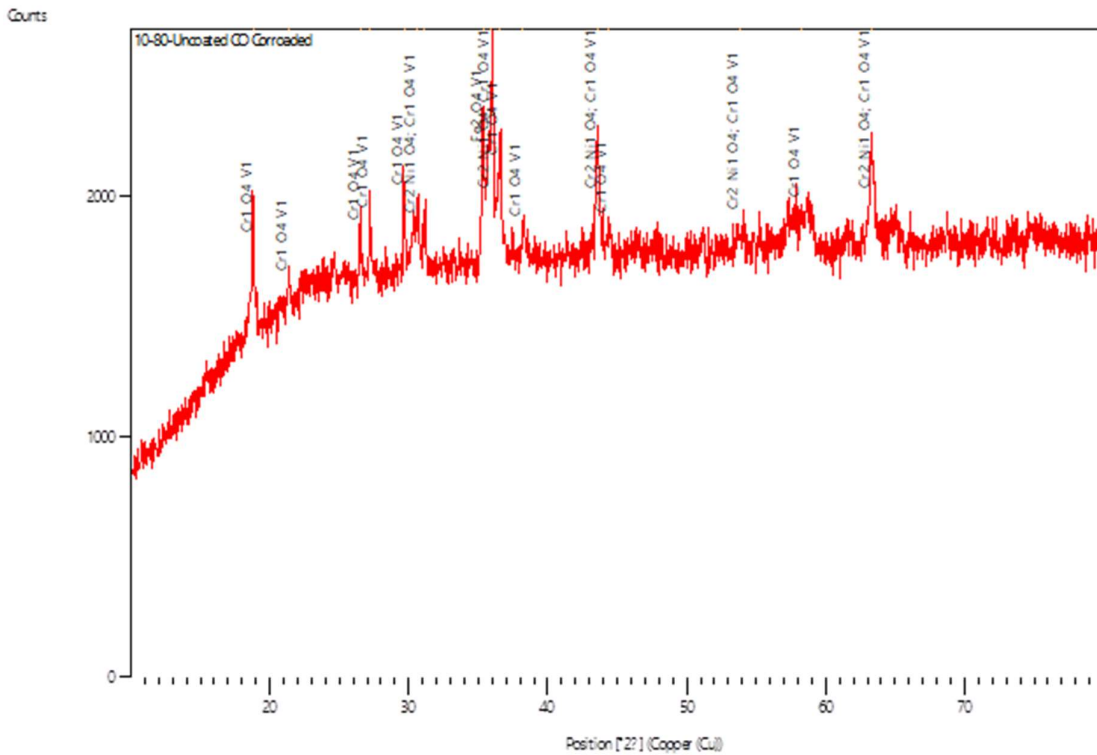


Fig.8. XRD patterns for uncoated Superco-605 subjected to hot corrosion at 700° C

- The coating of cermets WC-Co+ 70 Wt.% NiCrBSi on substrate Superco-605 is helpful in preventing penetration of reaction species in to substrate, and results in increased resistance against hot corrosion.

Acknowledgements

Acknowledgment: The authors extend their The authors wish to express their deep sense of gratitude to REVA University Bangalore for providing the lab facility to perform the Thermogravimetric study, and also express special thanks to VIGNYANA BHAVAN, and University of Mysore and SJCE, Mysore for providing SEM with EDS and XRD facility.

References

1. Kuruba, Manjunatha, et al. "Effect of carbon nanotubes on microhardness and adhesion strength of high-velocity oxy-fuel sprayed NiCr–Cr₃C₂ coatings." *Proceedings of the Institution of Mechanical Engineers, Part L: Journal of Materials: Design and Applications* 236.1 (2022) 86-96.
2. Singh, Amritbeer, et al. "Hot corrosion behaviour of different ceramics coatings on boiler tube steel at 800 C temperature." *Journal of Bio-and Tribo-Corrosion*. 7.1 (2021) 1-9.
3. Wang, Xu, et al. "Hot corrosion behavior of wire-arc sprayed NiCrB coatings." *Surface and Coatings Technology*. 367 (2019) 173-178.
4. Zhou, Wuxi, et al. "Hot corrosion behaviour of HVOF-sprayed Cr₃C₂-NiCrMoNbAl coating." *Surface and Coatings Technology*. 309(2017) 849-859.
5. Zhou, Wuxi, et al. "Hot corrosion behavior of HVOF-sprayed Cr₃C₂-WC-NiCoCrMo coating." *Ceramics International* 43.12(2017)9390-9400.
6. Sreenivasulu, V., and M. Manikandan. "Hot corrosion studies of HVOF sprayed carbide and metallic powder coatings on alloy 80A at 900° C." *Materials Research Express* 6.3 (2018) 036519.
7. Singh, Amritbeer, et al. "Hot corrosion behaviour of different ceramics coatings on boiler tube steel at 800 C temperature." *Journal of Bio-and Tribo-Corrosion*. 7.1 (2021) 1-9.
8. Wang, Xu, et al. "Hot corrosion behavior of wire-arc sprayed NiCrB coatings." *Surface*
9. Nithin, H. S., Desai Vijay, and M. R. Ramesh. "Cyclic oxidation and Hot Corrosion behavior of plasma-sprayed CoCrAlY+ WC-Co coating on turbine alloys." *Journal of Failure Analysis and Prevention* 18.5 (2018)1133-1142.
10. M S.Vinod Kumar., Suresh, R., and N. Jegadeeswaran. "Study of solid particle erosion behavior of HVOF spray coated superco-605 superalloy." *Materials Today: Proceedings* 45 (2021) 10-14.
11. Goyal, Khushdeep, Hazoor Singh, and Rakesh Bhatia. "Hot-corrosion behavior of Cr₂O₃-CNT-coated ASTM-SA213-T22 steel in a molten salt environment at 700° C." *International Journal of Minerals, Metallurgy, and Materials*. 26.3 (2019) 337-344.
12. Bhatia, Rakesh, Hazoor Singh Sidhu, and Buta Singh Sidhu. "High temperature behavior of Cr₃C₂-NiCr coatings in the actual coal-fired boiler environment." *Metallurgical and Materials Transactions E* 2.1 (2015) 70-86.

13. Babushkina, Elena A., et al. "Variation of the hydrological regime of Bele-Shira closed basin in Southern Siberia and its reflection in the radial growth of *Larix sibirica*." *Regional Environmental Change* 17.6 (2017) 1725-1737.
14. Mishra, N. K., Naveen Kumar, and S. B. Mishra. "Hot Corrosion Behaviour of Detonation Gun Sprayed Al₂O₃-40TiO₂ Coating on Nickel Based Superalloys at 900° C." *Indian Journal of Materials Science* 2014 (2014).
15. Khajezadeh, Mohammad Hossein, Majid Mohammadi, and Mojtaba Ghatee. "Hot corrosion performance and electrochemical study of CoNiCrAlY/YSZ/YSZ-La₂O₃ multilayer thermal barrier coatings in the presence of molten salt." *Materials Chemistry and Physics* 220 (2018) 23-34.
16. Kumar, Santosh, et al. "Performance of thermal-sprayed coatings to combat hot corrosion of coal-fired boiler tube and effect of process parameters and post-coating heat treatment on coating performance: a review." *Surface Engineering* 37.7 (2021) 833-860.
17. Muthu, S. M., M. Arivarasu, and N. Arivazhagan. "Investigation of hot corrosion resistance of bare and Ni-20% Cr coated superalloy 825 to Na₂SO₄-60% V₂O₅ environment at 900° C." *Procedia Structural Integrity* 14 (2019) 290-303.
18. Mehta, Jimmy, Varinder Kumar Mittal, and Pallav Gupta. "Role of thermal spray coatings on wear, erosion and corrosion behavior: a review." *Journal of Applied Science and Engineering* 20.4 (2017) 445-452.
19. Vasudev, Hitesh, et al. "A study on processing and hot corrosion behaviour of HVOF sprayed Inconel718-nano Al₂O₃ coatings." *Materials Today Communications* 25 (2020) 101626.
20. Sathishkumar, M., and M. Manikandan. "Hot corrosion behaviour of continuous and pulsed current gas tungsten arc welded Hastelloy X in different molten salts environment." *Materials Research Express* 6.12 (2019) 126553.
21. Kumar, Vinod, R. Suresh, N. Jegadeeswaran, and Meseret Leta Feyisa. "Experimental Investigation on the Effect of Coating Al₂O₃+ 70% NiCrBSi Cermets on Ti-31 Superalloy to Combat Hot Corrosion." *Journal of Nanomaterials* 2022 (2022).
22. Goyal, Khushdeep, Hazoor Singh, and Rakesh Bhatia. "Hot corrosion behaviour of carbon nanotubes reinforced chromium oxide composite coatings at elevated temperature." *Materials Research Express* 5.11 (2018) 116408.
23. Kumar, Sanjeet, et al. "Effect of CeO₂ in Cr₃C₂-NiCr coating on supermi 600 at high temperature." *Procedia materials science* 6 (2014) 939-949.
24. Yuan, Kang, et al. "Hot corrosion behavior of HVOF-sprayed CoNiCrAlYSi coatings in a sulphate environment." *Vacuum* 122 (2015) 47-53.
25. Singh, Karanjit, Khushdeep Goyal, and Rakesh Goyal. "Hot corrosion behaviour of different Cr₃C₂-NiCr coatings on boiler tube steel at elevated temperature." *World Journal of Engineering* (2019).
26. Singh, Sukhjinder, Khushdeep Goyal, and Rakesh Bhatia. "A review on protection of boiler tube steels with thermal spray coatings from hot corrosion." *Materials Today: Proceedings* (2022).

27. Jegadeeswaran, N., K. Udaya Bhat, and M. R. Ramesh. "Improving hot corrosion resistance of cobalt based superalloy (Superco-605) using HVOF sprayed oxide alloy powder coating." *Transactions of the Indian Institute of Metals* 68.2 (2015) 309-316.
28. Liu, Yu-Wan, et al. "Microstructures and corrosion behavior of HVOF-sprayed WC-12% Cr₃C₂-6% Ni coatings before and after sealing." *International Journal of Applied Ceramic Technology* 19.1 (2022): 383-396. Jegadeeswaran, N., et al. "Hot corrosion behavior of HVOF sprayed stellite-6 coatings on gas turbine alloys." *Transactions of the Indian Institute of Metals* 67.1 (2014) 87-93.
29. Kaushal, Gagandeep, et al. "Comparative high-temperature corrosion behavior of Ni-20Cr coatings on T22 boiler steel produced by HVOF, D-Gun, and cold spraying." *Metallurgical and Materials Transactions A* 45.1 (2014): 395-410.